

Biological and Structure-Activity Evaluation of Chalcone Derivatives against Bacteria and Fungi

Wender A. Silva,^{*,a} Carlos Kleber Z. Andrade,^{*,a} Hamilton B. Napolitano,^{a,b} Ivo Vencato,^{b,c} Carlito Lariucci,^c Miriam. R. C. de Castro^b and Ademir J. Camargo^b

^aLaQMOS, Instituto de Química, Universidade de Brasília, CP 4478, 70910-970 Brasília-DF, Brazil

^bCiências Exatas e Tecnológicas, Universidade Estadual de Goiás,
BR 153, km 98, 75133-050 Anápolis-GO, Brazil

^cInstituto de Física, Universidade Federal de Goiás, CP 131, 74001-970 Goiânia-GO, Brazil

O presente trabalho descreve as atividades antibacterianas e antifúngicas de diversas chalconas obtidas diretamente através da condensação aldólica tipo Claisen-Schmidt das quais se determinou a concentração inibitória mínima frente a diferentes microrganismos (bactérias Gram-positivas e Gram-negativas e fungos). Estruturas no estado sólido cristalino de sete chalconas foram determinadas por análise de difração de raios X (XRD). Estudos quimiométricos foram realizados com intuito de identificar uma potencial relação entre estrutura e atividade.

The present work describes the antibacterial and antifungal activities of several chalcones obtained by a straight Claisen-Schmidt aldol condensation determined by the minimal inhibitory concentration against different microorganisms (Gram-positive and Gram-negative bacteria and fungi). Solid state crystal structures of seven chalcones were determined by X-ray diffraction (XRD) analysis. Chemometric studies were carried out in order to identify a potential structure-activity relationship.

Keywords: chalcones, biological activities, X-ray structures, theoretical calculations

Introduction

Chalcone (1,3-diaryl-2-propen-1-ones) derivatives are found widespread in natural products from pteridophytes to highly organized multicellular organisms. This class of compounds is considered as key precursors for flavonoid and isoflavonoid syntheses¹ and can be directly obtained by aldol reactions under basic catalytic conditions. Chemically, they consist of open-chain flavonoids in which the two aromatic rings are joined by a three-carbon α,β -unsaturated carbonyl system (Figure 1). Studies on their multiple biological activities including anti-inflammatory,² anti-leishmania,³ antimitotic⁴ and antiviral are some few examples of their broad range of action.⁵ In particular, chalcone systems usually show different levels of inhibition during proliferative processes of a plethora of cancer cell lines.⁶

The presence of hydroxyl, allyl and prenyl groups in their structures commonly potentiates their activities.⁷

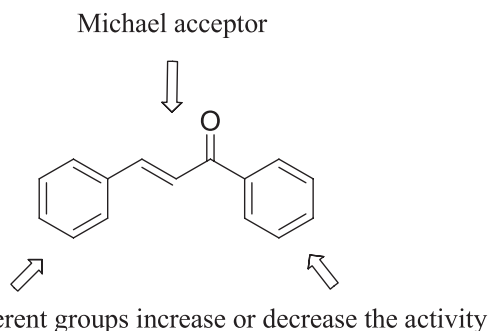


Figure 1. General structure of a chalcone.

For instance, the inclusion of two hydroxyl groups (dihydroxychalcones) enhanced both the antitumor and lipidic antiperoxidation activities.⁸ Other activities have already been reported⁹⁻¹¹ and Figure 2 shows some examples of biologically active chalcones.

Toxicity against several tumoral human cells¹² renders this class an attractive alternative to commonly used taxoid compounds, which are very complex structures of low

*e-mail: wender@unb.br; ckleber@unb.br

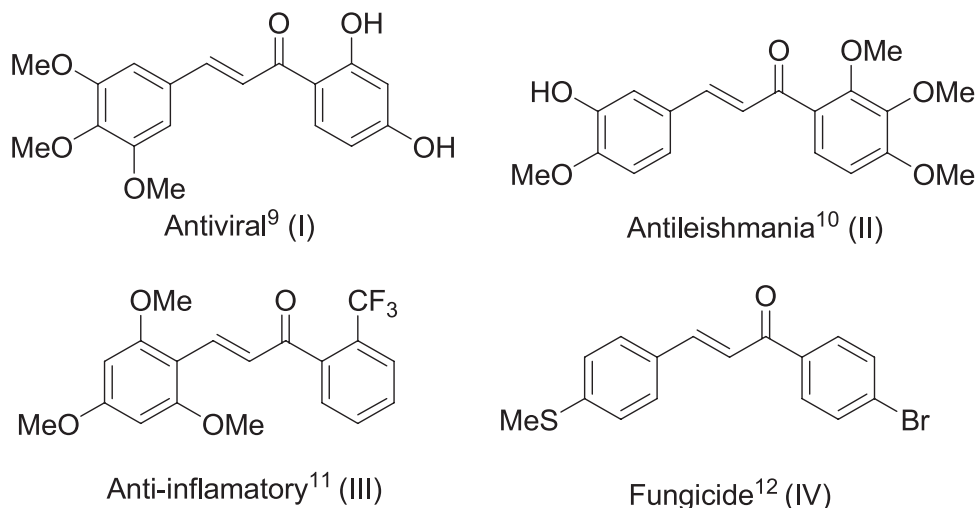


Figure 2. Some biologically active chalcone derivatives.

availability. Hence, the preparation and identification of simpler low-cost compounds such as chalcone derivatives for cytotoxic tests are still inexhaustible tasks aiming at the development of new and promising biologically active readily available molecules. As part of our ongoing studies on the synthesis, characterization and in silico studies of chalcone derivatives,¹³ it is described herein the preparation of 21 different chalcone derivatives, three of them (**3c**, **3f**, **3u**) are novel compounds, and their evaluation as antibacterial and antifungal agents upon determination of the minimal inhibitory concentration (MIC) against different microorganisms (Gram-positive and Gram-negative bacteria and fungi). Moreover, solid state crystal structures of seven chalcones were determined by X-ray diffraction (XRD) analysis. Theoretical calculation studies (structure modeling) were equally carried out in order to identify a potential structure-activity relationship.

Results and Discussion

Synthesis of chalcones

The chalcones were easily obtained from the aldol condensation of aromatic aldehydes and aromatic ketones¹⁴ (Table 1), in yields ranging from 70 to 100%. Chalcones **3a-g** are derived from 3,4-methylenedioxybenzaldehyde; chalcones **3h-i** from 4-nitrobenzaldehyde; chalcone **3j** from 4-(*N,N*-dimethylbenzaldehyde); chalcones **3k-l** from cinnamaldehyde; chalcones **3m-r** from benzaldehyde and finally chalcones **3s-u** from furfural. The chalcones were characterized by ¹H and ¹³C nuclear magnetic resonance (NMR) spectroscopy, X-ray diffractometry and elemental analyses (for the novel compounds). The ¹H NMR spectra showed two doublets between 7.0 and 8.0 ppm (J_{trans} 15-16 Hz) confirming the *trans* configuration of the

olefins whereas the carbonyl carbons appear in the range of 187.7 to 193.7 ppm in the ¹³C NMR spectra.

Due to the wide spectrum of action of this class of compounds and to their good cytotoxicity, our group began to investigate some structural modifications based on related studies in order to obtain molecules with potential biological activity. Allyl chalcones in particular were reported to exhibit widespread biological activities, with improved activities in some cases, probably due to their structural similarity to licochalcone E.⁷ In our group, studies were carried out in this way, and the allyl group was introduced into the structures of chalcones **3b**, **3n** and **3t**. Nevertheless, the insertions were not efficient, not reaching the expected activity.

Biological activity

Seven bacterial strains were used for testing antimicrobial activities, including Gram-positives: *Staphylococcus aureus* ATCC 6538, *Bacillus subtilis* ATCC 6833, *Streptococcus mutans* ATCC 25175, *Micrococcus luteus* ATCC 10240, and Gram-negatives: *Escherichia coli* ATCC 94863, *Pseudomonas aeruginosa* and *Salmonella choleraesuis* ATCC 14028. Three fungi were used: *Aspergillus niger* ATCC 16404, *Cladosporium cladosporioides* IMI 178517 and *Candida albicans* ATCC 18804. The results are summarized in Table 2 and indicate, in some cases, considerable activity against bacteria in comparison with the standard, especially for chalcones **3m**, **3n** and **3o**, which showed a good profile towards some microorganisms (e.g., chalcone **3n** on *S. mutans*). No activity at all was observed against the following microorganisms: *S. choleraesuis* ATCC 14028, *E. Coli* ATCC 94863 and *P. aeruginosa*.

In some cases, the activity is dependent on the substituents on the aromatic ring. For instance, chalcones

3m-q, obtained from benzaldehyde, showed distinct activities against *S. mutans* (Table 2). The best activity was achieved when the hydroxyl group resides on the *ortho* position (as in **3n**). In contrast, the activity is diminished in **3o** (OH in *meta* position) and in the absence of a substituent there was no activity. The protection of the hydroxyl group in **3n** as an allyl ether decreased the activity by two dilutions. Chalcones derived from furaldehyde (**3s-u**) were somewhat active but those derived from piperonal (**3a-g**) were inactive irrespective of the substituents on the aromatic ring.

When the fungi are concerned, *C. cladosporioides* was the most sensitive to the chalcones. The greatest activities were achieved by compounds **3a**, **3e** and **3k**. In the last two cases, the activities were at the same level of dilution as compared to Loprox[®], the standard drug used in the assay.

Crystallographic analysis

In order to get a better insight on the relationship between biological activity and structures, the crystal structure of seven chalcones were obtained for better

characterization. Figure 3 shows the ORTEP drawings of chalcones **3a**, **3f**, **3i**, **3n**, **3o**, **3q** and **3t** and the refinement data are shown in the Supplementary Information section.

Principal component analysis (PCA) of chalcones

The aim of this section is to get a relationship between geometric and electronic properties of the 21 synthesized chalcones and the biological activities against *S. aureus* ATCC 6538 and *C. cladosporioides* IMI 178517. For this purpose, quantum chemical calculations were carried out on chalcones and analogues, as listed in Table 1. The chalcones were tested against 10 microorganisms, but only two microorganisms were selected for this study, because the number of active and inactive chalcones for these two organisms is roughly equally distributed and this is very important for the statistical analysis of the calculated data to be meaningful, as shown in Table 3.

As can be seen in Figure 3, chalcones are chemical compounds with several rotational degrees of freedom and, in turn, they present many geometric conformations

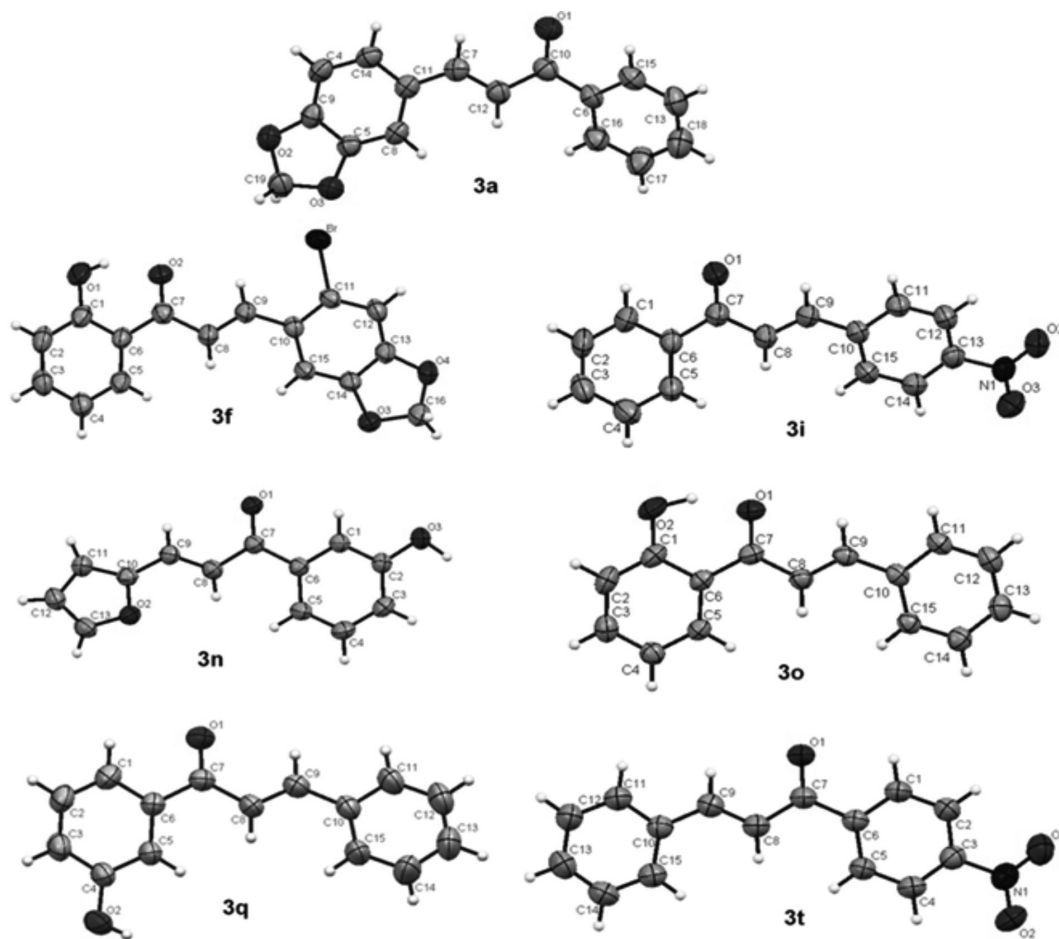


Figure 3. ORTEP drawings of chalcones **3a**, **3f**, **3i**, **3n**, **3o**, **3q** and **3t**, with the atom-numbering schemes. The displacement ellipsoids are drawn at the 30% probability levels.

Table 1. Synthesis of chalcones and analogues **3a-3u**

Compound	Chalcone	R ¹	R ²	R ³	R ⁴	Yield / %
3a		H	H	H	H	92
3b		H	OH	H	H	81
3c		H	O(allyl)	H	H	100
3d		H	H	H	OMe	90
3e		H	H	H	NO ₂	84
3f		Br	OH	H	H	80
3g		H	H	H	Ph	85
3h		-	-	-	NO ₂	70
3i		-	-	-	H	85
3j		-	-	-	NO ₂	90
3k		-	-	-	H	90
3l		-	-	-	NO ₂	85
3m		-	H	H	H	80
3n		-	OH	H	H	84
3o		-	H	OH	H	83
3p		-	H	H	OMe	80
3q		-	H	H	NO ₂	82
3r		-	O(allyl)	H	H	100
3s		-	-	H	-	96
3t		-	-	OH	-	88
3u		-	-	O(allyl)	-	100

that are energetically stable. For this reason, it is mandatory to carry out a conformational search to find the molecular conformation with the lowest energy. In this work, the conformational searches were carried out using HyperChem™ 7.5 suite of programs¹⁵ with semiempirical quantum method PM3^{16,17} and random walk algorithm. Initially, the most active chalcone was analyzed and the most stable conformation was selected. Afterwards, the remaining chalcones were investigated and the energetically most stable conformation that was similar to the conformation selected before was chosen for the calculation of the molecular properties. Before calculating the properties, the molecular geometries were optimized

again, but now using the density functional theory (DFT)^{18,19} with the hybrid exchange-correlation functional B3LYP²⁰⁻²² and the basis set 6-31G(d) as implemented in the software package G09²³, which was also used to calculate the molecular properties (descriptors or variables). In this work, the following molecular descriptors were calculated: HOMO-1 (second highest occupied molecular orbital energy), HOMO (highest occupied molecular orbital energy), LUMO (lowest unoccupied molecular orbital energy), LUMO+1 (second lowest unoccupied molecular orbital energy), partition coefficient (logP) (this property was obtained from the hydrophobic parameters of the substituents using HyperChem™ 7.5), Mulliken

Table 2. Activities (MICs) of the chalcones against bacteria and fungi

Samples / ($\mu\text{g mL}^{-1}$)	Microorganisms									
	<i>B. subtilis</i> ATCC 6633	<i>S. aureus</i> ATCC 6538	<i>M. luteus</i> ATCC 10240	<i>S. mutans</i> ATCC 25175	<i>S. choleraesuis</i> ATCC 14028	<i>E. coli</i> ATCC 94863	<i>P. aeruginosa</i>	<i>C. albicans</i> ATCC 18804	<i>A. niger</i> ATCC 16404	<i>C. cladosporioides</i> IMI 178517
3a	>100	100	100	>100	>100	>100	>100	>100	>100	12.5
3b	>100	>100	>100	>100	>100	>100	>100	>100	50	> 100
3c	>100	50	100	100	>100	>100	>100	100	>100	> 100
3d	>100	100	>100	100	>100	>100	>100	>100	100	100
3e	>100	> 100	>100	>100	>100	>100	>100	>100	>100	6,3
3f	>100	>100	>100	>100	>100	>100	>100	>100	100	> 100
3g	>100	>100	>100	>100	>100	>100	>100	>100	>100	> 100
3h	>100	>100	>100	100	>100	>100	>100	>100	>100	> 100
3i	>100	>100	>100	>100	> 100	> 100	> 100	> 100	> 100	>100
3j	>100	>100	>100	>100	>100	>100	>100	>100	>100	> 100
3k	>100	>100	>100	>100	>100	>100	>100	100	>100	6.3
3l	>100	>100	100	>100	> 100	> 100	> 100	> 100	> 100	> 100
3m	>100	25	100	100	>100	>100	>100	50	>100	25
3n	100	25	25	12,5	>100	>100	>100	100	>100	25
3o	50	25	25	25	>100	>100	>100	50	100	100
3p	>100	100	100	>100	>100	>100	>100	>100	>100	> 100
3q	>100	>100	>100	>100	>100	>100	>100	>100	>100	> 100
3r	>100	100	100	50	>100	>100	>100	>100	>100	> 100
3s	>100	100	100	100	>100	>100	>100	>100	>100	50
3t	50	100	50	50	>100	>100	>100	>100	>100	100
3u	> 100	50	100	50	>100	>100	>100	50	>100	> 100
Chloramphenicol	6.3	6.3	0.78	6.3	6.3	3.1	100	–	–	–
Loprox®	–	–	–	–	–	–	–	6.3	12.5	6.3

Table 3. Theoretical values for the selected descriptors used in the PCA analysis for the activities against *C. cladosporioides* and *S. aureus*. The activities are also included

Chalcone	<i>C. cladosporioides</i>				<i>S. aureus</i>			
	AD _{1,2,3,4}	PsiH-13	Ref	Activity	b _{7,14}	PsiL-2	A _{12,2,3}	Activity
3a	-174.90	0.00	72.64	active	0.9023	11.76	118.126	active
3b	173.37	0.00	68.50	inactive	1.1184	9.075	118.338	inactive
3c	174.92	0.00	74.32	inactive	0.8945	6.371	119.975	active
3d	-175.08	0.00	88.27	active	0.9063	11.187	118.131	active
3e	176.37	0.00	74.34	active	0.9053	10.078	117.849	inactive
3f	174.09	0.00	68.57	inactive	0.8950	14.336	118.198	inactive
3g	174.07	0.00	73.34	inactive	0.9005	20.293	118.183	inactive
3h	175.27	0.00	74.20	inactive	0.8982	4.842	118.25	inactive
3i	178.39	0.02	82.50	inactive	1.0147	18.849	117.72	inactive
3j	174.69	0.00	58.69	inactive	0.9024	11.011	120.045	inactive
3k	-174.43	0.00	79.11	active	0.9005	9.531	118.135	inactive
3l	174.43	0.00	60.39	inactive	0.9015	9.908	120.039	inactive
3m	-175.58	0.00	79.97	active	0.8984	2.275	118.204	active
3n	177.96	0.06	81.89	active	1.1188	15.108	116.365	active
3o	-179.18	0.24	97.78	active	0.8974	2.532	116.038	active
3p	178.83	0.22	82.89	inactive	0.8916	3.368	117.105	active
3q	-174.68	0.00	81.53	inactive	0.8974	2.286	118.482	inactive
3r	-173.97	0.05	74.20	inactive	0.9014	5.034	118.433	active
3s	-175.92	0.00	88.56	active	0.8990	3.542	117.913	active
3t	-179.97	0.00	75.56	active	0.8967	10.289	117.424	active
3u	-175.92	0.00	66.88	inactive	0.9022	20.97	117.913	active

electronegativity ($\chi = (E_{\text{HOMO}} - E_{\text{LUMO}})/2$), dipole moment, molecular polarizability, total electronic energy, heat of formation, electron affinity (obtained as $-E_{\text{HOMO}}$), band gap energy ($E_{\text{LUMO}} - E_{\text{HOMO}}$), hardness, softness, molar refractivity index, ionization potential energy, net atomic charge on atom derived from electrostatic potential, molecular area, molecular volume, bond order, bond length between adjacent atoms, angles between three consecutive atoms, dihedral angles between four consecutive atoms, molecular length, hydration energy, $\text{Psi} - x = \sum_i |c_{i\text{HOMO}}|^2$ and $\text{Psi} - x = \sum_i |c_{i\text{LUMO}}|^2$, where x stands for atom number as shown in Figure 4.

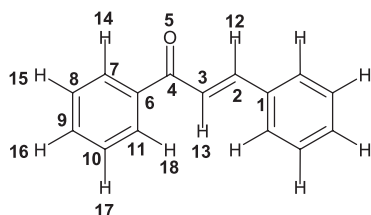


Figure 4. Atomic numbering used in the calculations of the molecular descriptors.

The frontier electron reactivity theory, which explains many organic reactions, states that the reaction between two reactants takes place where the overlap of HOMO and LUMO is maximized.²⁴ The HOMO density ($\text{PsiH}-x$) is closely related to the charge transfer (nucleophilic reactant), while for an acceptor compound the LUMO density ($\text{PsiL}-x$) is important (electrophilic reactant). A total of 118 geometrical and electronic molecular descriptors was obtained from *ab initio* calculations in such a way that they can represent electronic, steric and hydrophobic features of the chalcones. These features are supposed to be important to elucidate the biological activity of the chalcones against *S. aureus* ATCC 6538 and *C. cladosporioides* IMI 178517.

In order to find a relationship between the calculated descriptors and the biological activities, an analysis using the multivariate statistical was carried out using the Einsight program.²⁵ At the outset, the Fisher weight²⁶ for each descriptor was calculated in order to discriminate those variables that are the most important to separate the active from the inactive chalcones. The Fisher weight (w_k) for the variable k was obtained from the following equation 1:

$$w_k(\text{active, inactive}) = \frac{(\bar{x}_{\text{active}} - \bar{x}_{\text{inactive}})^2}{(1/N_{\text{active}})\sum(x_{\text{active}} - \bar{x}_{\text{active}})^2 + (1/N_{\text{inactive}})\sum(x_{\text{inactive}} - \bar{x}_{\text{inactive}})^2} \quad (1)$$

In this equation, \bar{x}_{active} and $\bar{x}_{\text{inactive}}$ are the mean values for the active and inactive molecules and $(1/N_{\text{active}})\sum(x_{\text{active}} - \bar{x}_{\text{active}})^2$ and $(1/N_{\text{inactive}})\sum(x_{\text{inactive}} - \bar{x}_{\text{inactive}})^2$ are the respective variances. Those descriptors with high Fisher weights are more significant to discriminate the

compounds between active and inactive, allowing, in this way, a reduction in the number of variables to be used in PCA.

The major aim in the PCA technique is to reduce the dimensionality of the data set to lower dimensional space for analysis.²⁷ This is achieved through an orthogonal linear transformation of the original data set of descriptors into a smaller set of uncorrelated significant principal components (PCs). This transformation can be seen as a rotation of the original coordinate system in such a way that the first principal component (PC1) axis describes the maximum variance of the data set. The second principal component (PC2), which is orthogonal to the first one, describes the second maximum variance and so on. In general, the great majority of the variance of the data set is described by the first components and can be utilized to represent the entire data set in a simplified way. For this reason, principal component analysis is a useful tool for helping in the visualization of hidden patterns, providing descriptive models. *A priori*, all descriptors are likewise important to explain the biological activity. So, before applying PCA technique, the data were auto-scaled, i.e., each variable was mean centered and divided by standard deviation, so each variable in the matrix data can be compared to each other on the same scale. The auto-scaling procedure was calculated according to equation 2,

$$x_{ik} = (x_i - \bar{x}_i) / \sqrt{\sigma_i^2} \quad (2)$$

where x_{ik} represents the auto-scaled variable i for the sample k , $\sqrt{\sigma_i^2}$ stands for standard deviation and \bar{x}_i is the mean value of the variable i .

Activity against *C. cladosporioides* IMI 178517

The atomic numbering used in the calculation of the molecular descriptors is shown in Figure 4. After several attempts to separate the active from the inactive chalcones against *C. cladosporioides* IMI 178517, the best result was finally obtained with three descriptors: dihedral angle between atoms 1, 2, 3, and 4 (DA1,2,3,4), ($\text{PsiH}-13$), and refractive index (Ref) (the names in parenthesis represent the names of the respective descriptors plotted in Figure 5). Figure 6 shows the score plots. Observe that two components (PC1 and PC2) are necessary to discriminate the chalcones into active and inactive. These two principal components together explain 89.33% of the total variance in the data set as follows: PC1 = 56.32% and PC2 = 33.01%. The amount of total variance explained in the data set by these two components represents very well the higher order space. The score plot in Figure 6 shows that the

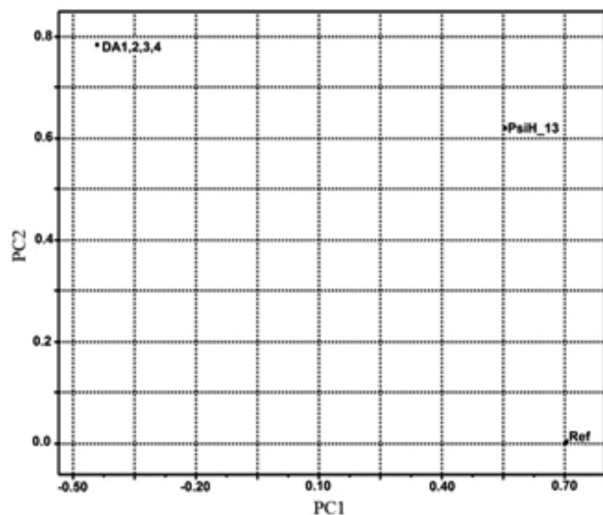


Figure 5. Plot showing the descriptor loadings, which explain the activity of the compounds against *C. cladosporioides*. DA1,2,3,4 stands for dihedral angle among the atoms 1, 2, 3 and 4, PsiH-13 represents the HOMO density on atom 13 and Ref stands for molecular refractive index.

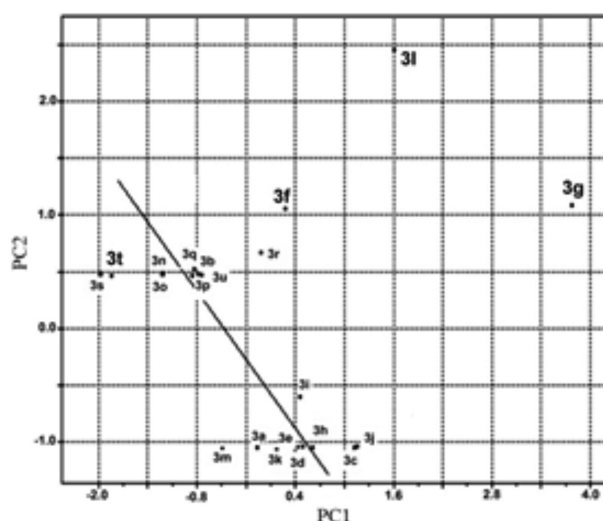


Figure 6. Plot showing the scores for the activity of the chalcone derivatives against *C. cladosporioides*. It is worth noting that all the active compounds (3a, 3d, 3e, 3k, 3m, 3n, 3o, 3s and 3t) stand below the solid line drawn in figure.

active chalcones against *C. cladosporioides* are gathered below the solid line drawn in the figure. The mathematic representations for these two components are expressed through equations 3 and 4.

$$PC1 = 0.7046 \text{ Ref} + 0.5552 \text{ PsiH} - 13 - 0.4419 \text{ DA}_{1,2,3,4} \quad (3)$$

$$PC2 = 0.0033 \text{ Ref} + 0.6202 \text{ PsiH} - 13 - 0.7845 \text{ DA}_{1,2,3,4} \quad (4)$$

From analysis of equations 3 and 4, it is possible to see that the variable Ref is not meaningful in the second component but is very important in the first component. The other descriptors, namely PsiH-13 and dihedral angle between atoms 1, 2, 3, and 4 (DA1,2,3,4) are important in

both components. For a chalcone to be classified as active against *C. cladosporioides*, it must stand below the solid line drawn in Figure 6. This means that the scores for both components should be small and, in turn, for the scores to be small, the variables Ref and PsiH-13 should present lower values. However, as shown in equations 3 and 4, the situation for the variable DA1,2,3,4 is a little delicate because it should present higher value in the first component (the loading is negative for this variable in PC1) and lower value in the second one (the loading is positive) in order to help in the discrimination of the compounds. As shown in Table 3, the value of this dihedral angle is almost 180°, which means that the chalcones are almost planar in this molecular region. PsiH-13 describes the HOMO density on atom 13 and, according to equations 1 and 2, it should have lower values in order to help in the discrimination of the compounds. From these observations, it is possible to hypothesize the three major characteristics for a chalcone to be active: (i) lower values of refractive index (Ref), (ii) lower values of the HOMO density on atom 13 (PsiH-13) (see Figure 4 for the numbering), and (iii) intermediate values of dihedral angle between the atoms 1, 2, 3 and 4 (DA1,2,3,4). These molecular characteristics can help us to design new chalcones with activity against *C. cladosporioides*.

Activity against *S. aureus* ATCC 6538

The active chalcones against *S. aureus* ATCC 6538 stand above the solid line drawn in Figure 7. As can be noted in this figure, only one component (PC2) is needed to separate the active chalcones from the inactive ones. The component PC2 accounts for 33.02% of the total variance of the original data, while the first component (PC1) accounts for 46.62%. Both components added up to 79.64% of the total variance in the original data. A close look in equation 5 and in Figure 8 shows that the descriptors responsible for the discrimination are the angle between atoms 12, 2 and 3 (A12-2-3), PsiL-2, and bond order between atoms 7 and 14 (b7,14). Equation 5 also shows that for a compound to fall in the active group, it should present higher values of PsiL-2 and A12-2-3 variables. The bond order b7-14 is not important in this component, but to run the EInsight program,²⁵ it was necessary to include it in the calculation.

$$PC1 + 0.001b7.14 + 0.694\text{PsiL}2 + 0.720\text{A12,2,3} \quad (5)$$

As pointed out before, the variable PsiL-2 is closely related to the importance of the atom 2 in the lowest unoccupied molecular orbital (LUMO). Equation 5 shows that this descriptor should be higher for the molecule to be active. That may mean that the atom 2 (Figure 4) could be

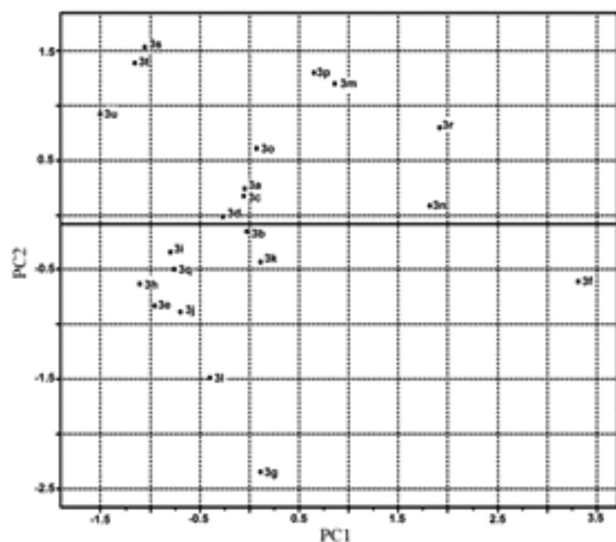


Figure 7. Plot showing the scores for the activity of the compound derivatives against *S. aureus*. Note that all the active compounds stand above the solid line drawn in figure.

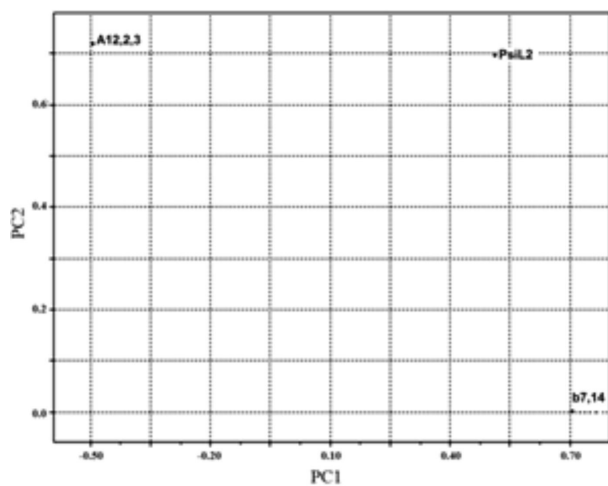


Figure 8. Graphic representation of variable loadings (A12,2,3, PsiL-2, b7,14) that discriminate the active from the inactive chalcones against *S. aureus*.

involved in the formation of some kind of chemical bond in the structure of *S. aureus* ATCC 6538. From that discussion, it is possible to postulate that the chalcones studied need to present two main characteristics to express activity against *S. aureus* ATCC 6538: (i) they must have a large angle between atoms 12, 2 and 3 (A12,2,3), and (ii) they need to increase the value of LUMO density, which is probably related to some kind of reaction in expressing their activities. This characteristic can be useful in designing compounds with activity against *S. aureus* ATCC 6538.

Conclusions

A series of chalcones was prepared and evaluated against bacteria and fungi. Some compounds showed

promising activity against *C. cladosporioides*, with low inhibitory values, in some cases in the same order of magnitude as the standard (Loprox®). Chemometric studies were employed to find a possible structure-activity relationship and allowed to establish some important features for the chalcones to be active. For instance, the best activity against *C. cladosporioides* IMI 178517 was obtained with three descriptors: dihedral angle between atoms, HOMO density on atom 13 (PsiH-13) and refractivity index (Ref) and two components (PC1 and PC2) were necessary to discriminate the chalcones into active and inactive. In the case of *S. aureus* ATCC 6538, only one component (PC2) was needed and the descriptors responsible for the discrimination were the bond angle (A12-2-3), PsiL-2, and bond order between atoms (b7,14). Future efforts to optimize the structures of this class of compounds may involve design, as well as the study of the effect of some groups strategically placed in positions in the structure of chalcones that may influence some properties such as solubility.

Experimental

General

All reagents were obtained from Sigma-Aldrich and used without purification. ¹H NMR spectra were recorded at 300 MHz on a Varian Mercury Plus 7.04 T spectrometer and chemical shifts were reported relative to internal Me₄Si. ¹³C NMR spectra were recorded at 75 MHz on a Varian Mercury Plus 7.04 T spectrometer and chemical shifts were reported relative to internal CDCl₃. The infrared spectra were obtained on a Bomem MB-100 spectrometer. Elemental analyses were obtained on a Perkin Elmer series II CHNS/O Analyzer 2400.

General synthetic procedure for chalcones

The ketone (1 mmol) was added to a solution of NaOH (10% m/v) and ethanol (3 mL) and the mixture was stirred for 20 min under ice bath cooling. Then, the aldehyde (1 mmol) was added and the resulting mixture was stirred overnight at room temperature. The reaction mixture was acidified with 10% HCl. The precipitate was collected, washed with cold water, dried and purified by recrystallization from EtOH or in appropriate solvents (generally chloroform and methylene chloride). The chalcones that did not crystallize were washed with chloroform and purified by column chromatography (20% ethyl acetate/hexane).

MIC assays

The determinations of MIC were performed essentially according to the National Committee for Clinical Laboratory Standards (NCCLS)²⁸ as described by Ellof²⁹ and Kusucu *et al.*³⁰ The microorganisms were obtained from the Fundação Tropical de Pesquisa e Tecnologia André Tosello, Campinas-SP, Brazil, with exception of *E. coli* and *P. aeruginosa*, obtained from Departamento de Farmácia of Universidade Federal da Bahia, Salvador-BA, Brazil. The bacteria were grown for 24 h at 35 °C on nutrient agar. The fungi and yeast were cultivated for 72 h at 26 °C on malt extract agar and yeast malt agar, respectively. The inocula for the assays were prepared by cell suspensions according to McFarland scale 0.5 (108 CFU mL⁻¹).

To determine MIC of the compounds against the microorganisms, the following modified micro dilution method was carried out: the compounds were dissolved in sterile dimethyl sulfoxide (2000 mg mL⁻¹) and 20 µL of the stock solutions were transferred into 96 well sterile microtiter plates. Then, serial dilutions with nutrient broth to bacteria and malt extract broth to fungi were performed, so that the concentrations of the tested compounds ranged from 100 to 0.78 mg mL⁻¹. Finally, an aliquot (100 µL) of culture medium containing the microorganism suspension was added to the wells. Chloramphenicol and Loprox[®] were used as the reference drugs against bacteria and fungi, respectively, and DMSO was used as negative control. The plates were incubated at 35 °C for 24 h to bacteria and fungi and yeast were maintained at 26 °C for 72 h. After incubation, an aliquot of 50 µL of aqueous [3-(4,5-dimethyl-2-tiazolyl)-2,5 diphenyl-2H-tetrazolium bromide] (MTT at 0.05%) was added on the wells and the reduction of tetrazolium salt (yellow) from (blue) indicated the presence of viable cells. MIC is defined as the lowest concentration of the substances which inhibited the growth of the microorganisms.

Crystallographic structure determinations of compounds **3a**, **3f**, **3i**, **3n**, **3o**, **3q** and **3t**

Single crystal X-ray diffraction data were collected at room temperature using a Nonius CAD-4 diffractometer³¹ and using Cu K_α radiation (λ = 1.54180 Å). The structures were solved by direct methods and anisotropically refined with full-matrix least-squares on F² using SHELXL97.³² The hydrogen atoms were placed at calculated position except those involved in H-bonds and weak interactions found on difference maps and refined with riding constraints. With regard to the hydrogen atoms, those bonded to carbon atoms were placed in expected positions according to the

stereochemical predictions. They were refined with fixed individual displacement parameters 20% greater than the equivalent isotropic displacement parameter of the corresponding carbon atom. Aromatic C-H bond distances were fixed according to the riding model (0.93 Å). The (x, y, z) fractional coordinates and the isotropic thermal parameter of these H atoms were not constrained during refinements. The Mercury³³ and ORTEP-3³⁴ programs were used within the WinGX³⁵ software package to deal with the processed crystallographic data and artwork representations. The conformational and geometric features of this molecule were checked comparing with other similar structures. The crystallographic data for compounds **3f**, **3i**, **3a**, **3n** and **3t** were deposited at the Cambridge Crystallographic Data Center under the numbers 819655, 819656, 819657, 819681 and 823762, respectively.

The respective solutions, anisotropic refinements, geometrical calculations, molecular packing and drawings were performed using the program package WINGX. (**3a**): C₁₆H₁₂O₃, *a* = 7.809(2), *b* = 11.1764(9), *c* = 28.601(2) Å, orthorhombic system, space group Pcab, *R* = 0.0557; (**3f**): C₁₆H₁₁O₄Br, *a* = 4.160(3), *b* = 11.757(2), *c* = 27.598(7) Å, β = 92.87(4)°, monoclinic system, space group P21/c, *R* = 0.0809; (**3i**): C₁₅H₁₁NO₃, *a* = 4.7580(9), *b* = 6.096(1), *c* = 10.658(2) Å, α = 95.807(2)°, β = 90.482(2)°, γ = 96.397(2)°, triclinic system, space group P1, *R* = 0.0492; (**3t**): C₁₃H₁₀O₃, *a* = 3.9530(9), *b* = 14.583(2), *c* = 17.893(5) Å, monoclinic, space group P21/n, *R* = 0.0527; (**3o**): C₁₅H₁₂O₂; *a* = 12.641(1), *b* = 12.066(2), *c* = 7.813(1) Å, β = 101.278(9)°, monoclinic system, space group P21/c, *R* = 0.0820; (**3n**): C₁₅H₁₂O₂, *a* = 6.822(2), *b* = 10.474(4), *c* = 17.097(2) Å, α = 73.88(2), β = 84.29(2), γ = 87.66(3)°. Triclinic, space group P-1, *R* = 0.0701; (**3q**): C₁₅H₁₁NO₃, *a* = 6.299(3), *b* = 13.226(3), *c* = 14.809 Å, β = 99.73(9)°, monoclinic system, space group P21/c, *R* = 0.0660.

Spectroscopic data for the chalcones

(2*E*)-3-(1,3-Benzodioxol-5-yl)-1-phenylprop-2-en-1-one (**3a**):³⁶ IR (KBr) ν_{max}/cm⁻¹ 3021, 2928, 1660, 1598, 1503, 1310, 1104, 770, 686; ¹H NMR (300 MHz, CDCl₃) 8.02-7.98 (m, 2H), 7.73 (d, 1H, *J* 15.7 Hz), 7.61-7.46 (m, 3H), 7.36 (d, 1H, *J* 15.7 Hz), 7.16 (d, 1H, *J* 1.4 Hz), 7.11 (dd, 1H, *J* 8.1 and 1.9 Hz), 6.84 (d, 1H, *J* 8.1 Hz), 6.02 (s, 2H); ¹³C NMR (75 MHz, CDCl₃) 190.4, 149.9, 148.4, 144.7, 138.3, 132.6, 129.3, 128.5, 128.4, 125.2, 120.0, 108.6, 106.6, 101.6.

(*E*)-3-(Benzo[d][1,3]dioxol-6-yl)-1-(2-hydroxyphenyl)prop-2-en-1-one (**3b**):³⁶ ¹H NMR (300 MHz, CDCl₃) 12.90

(s, 1H), 7.90 (dd, 1H, *J* 6.6 and 1.4 Hz), 7.85 (d, 1H, *J* 15.3 Hz), 7.50 (d, 1H, *J* 15.3 Hz), 7.52-7.47 (m, 1H), 7.18 (dd, 1H, *J* 6.9 and 1.7 Hz), 7.14 (d, 1H, *J* 1.45 Hz), 7.03 (dd, 1H, *J* 8.4 and 0.9 Hz), 6.97-6.91 (m, 1H), 6.82 (d, 1H, *J* 8.1 Hz), 6.05 (s, 2H); ¹³C NMR (75 MHz, CDCl₃) 193.5, 163.5, 150.3, 148.5, 145.3, 136.2, 129.5, 129.0, 125.7, 120.0, 118.8, 118.6, 117.9, 108.7, 106.7, 101.7.

(*E*)-1-(2-(allyloxy)phenyl)-3-(benzo[d][1,3]dioxol-6-yl)prop-2-en-1-one (**3c**): ¹H NMR (300 MHz, CDCl₃) 7.64 (dd, 1H, *J* 7.4 and 1.8 Hz), 7.56 (d, 1H, *J* 15.7 Hz), 7.47-7.41 (m, 1H), 7.30 (d, 1H, *J* 15.7 Hz), 7.09-6.96 (m, 4H), 6.81 (d, 1H, *J* 7.8 Hz), 6.10-5.97 (m, 3H), 5.42 (dq, 1H, *J* 3.0 and 1.5 Hz), 5.26 (dq, 1H, *J* 3.0 and 1.5 Hz); ¹³C NMR (75 MHz, CDCl₃) 192.5, 157.0, 149.5, 148.2, 142.6, 132.7, 132.5, 130.4, 129.7, 129.5, 125.2, 124.9, 120.9, 117.6, 112.8, 108.5, 106.5, 101.5, 69.2 anal. calcd. for C₁₆H₁₄O₃: C, 75.57; H, 5.55; O, 18.88; found: C, 75.48; H, 5.51; O, 19.01.

(*E*)-3-(Benzo[d][1,3]dioxol-6-yl)-1-(4-methoxyphenyl)prop-2-en-1-one (**3d**):³⁶ ¹H NMR (300 MHz, CDCl₃) 7.99-8.05 (m, 2H), 7.73 (d, 1H, *J* 15.6 Hz), 7.38 (d, 1H, *J* 15.9 Hz), 7.17 (d, 1H, *J* 1.9 Hz), 7.11 (dd, 1H, *J* 8.4 and 1.9 Hz), 6.95-7.00 (m, 1H), 6.83 (d, 2H, *J* 7.8 Hz), 6.02 (s, 2H), 3.88 (s, 3H); ¹³C NMR (75 MHz, CDCl₃) 188.5, 163.3, 149.7, 148.3, 143.8, 131.2, 130.7, 129.5, 125.0, 119.9, 113.8, 108.6, 106.6, 101.6, 55.5.

(*E*)-3-(Benzo[d][1,3]dioxol-6-yl)-1-(4-nitrophenyl)prop-2-en-1-one (**3e**):³⁶ ¹H NMR (300 MHz, CDCl₃) 8.37-8.32 (m, 2H), 8.15-8.11 (m, 2H), 7.78 (d, 1H, *J* 15.4 Hz), 7.31 (d, 1H, *J* 15.4 Hz), 7.18-7.13 (m, 2H), 6.88 (d, 1H, *J* 8.1 Hz), 6.06 (s, 2H); ¹³C NMR (75 MHz, CDCl₃) 188.8, 150.7, 150.6, 148.6, 146.7, 143.3, 129.3, 128.8, 126.0, 123.9, 119.2, 108.8, 106.7, 101.8.

(*E*)-3-(4-Bromobenzo[d][1,3]dioxol-5-yl)-1-(2-hydroxyphenyl)prop-2-en-1-one (**3f**): ¹H NMR (300 MHz, CDCl₃) 12.80 (s, 1H), 8.23 (d, 1H, *J* 15.6 Hz), 7.88 (dd, 1H, *J* 8.1 and 1.7 Hz), 7.53-7.47 (m, 1H), 7.44 (d, *J* 15.6 Hz), 7.23 (s, 1H), 7.10 (s, 1H), 7.03 (dd, 1H, *J* 8.1 and 1.7 Hz), 6.97-6.91 (m, 1H), 6.06 (s, 2H); ¹³C NMR (75 MHz, CDCl₃) 193.3, 163.6, 150.6, 148.0, 143.7, 136.4, 129.6, 127.9, 120.7, 119.9, 118.9, 118.7, 113.4, 106.5, 102.4. Anal. Calcd. for C₁₆H₁₁BrO₄: C, 55.36; H, 3.19. Found: C, 55.25; H, 3.16.

(*E*)-3-(Benzo[d][1,3]dioxol-6-yl)-1-(4-phenyl)prop-2-en-1-one (**3g**):³⁷ ¹H NMR (300 MHz, CDCl₃) 8.11-8.08 (m, 2H), 7.78 (d, 1H, *J* 15.7 Hz), 7.74-7.64 (m, 4H), 7.51-7.38 (m, 3H), 7.43 (d, *J* 15.7 Hz, 1H), 7.20 (d, 1H, *J* 1.8 Hz),

7.15 (dd, 1H, *J* 8.0 and 1.4 Hz), 6.85 (d, 1H, *J* 8.0 Hz), 6.03 (s, 2H); ¹³C NMR (75 MHz, CDCl₃) 189.7, 149.9, 148.4, 145.4, 144.6, 139.9, 137.0, 129.4, 129.0, 128.9, 128.1, 127.3, 127.2, 125.3, 119.9, 108.7, 106.7, 101.6.

(*E*)-1,3-bis(4-nitrophenyl)prop-2-en-1-one (**3h**):³⁸ ¹H NMR (300 MHz, CDCl₃) 8.41-8.37 (m, 1H), 8.34-8.28 (m, 3H), 8.21-8.16 (m, 2H), 7.91-7.81 (m, 3H), 7.61 (d, 1H, *J* 15.5 Hz); ¹³C NMR (75 MHz, CDCl₃) 188.2, 143.4, 142.2, 140.3, 129.5, 129.4, 129.2, 124.7, 124.3, 124.2, 124.0, 123.8.

(*E*)-3-(4-Nitrophenyl)-1-phenylprop-2-en-1-one (**3i**):³⁹ ¹H NMR (300 MHz, CDCl₃) 8.30-8.25 (m, 2H), 8.06-8.02 (m, 2H), 7.85-7.75 (m, 3H), 7.82 (d, 1H, *J* 15.6 Hz); ¹³C NMR (75 MHz, CDCl₃) 189.6, 148.5, 141.4, 141.0, 137.4, 133.3, 128.9, 128.8, 128.5, 125.6, 124.1.

(*E*)-3-(4-(Dimethylamino)phenyl)-1-(4-nitrophenyl)prop-2-en-1-one (**3j**):⁴⁰ ¹H NMR (300 MHz, CDCl₃) 8.38-8.31 (m, 2H), 8.15-8.09 (m, 2H), 7.82 (d, 1H, *J* 15.3 Hz), 7.58-7.54 (m, 2H), 7.27 (d, 1H, *J* 15.3 Hz), 6.73-6.69 (m, 2H); ¹³C NMR (75 MHz, CDCl₃) 188.9, 152.3, 149.6, 147.8, 144.2, 130.9, 129.1, 123.7, 122.2, 116.0, 111.9, 40.2.

(*E*,*E*)-1,5-Diphenylpenta-2,4-dien-1-one (**3k**):⁴¹ IR (film) ν_{\max} /cm⁻¹ 3059, 3027, 1676, 1594, 1448, 1034, 776, 700; ¹H NMR (300 MHz, CDCl₃) 8.03-7.93 (m, 2H), 7.63-7.22 (m, 10H), 7.13-6.92 (m, 2H); ¹³C NMR (75 MHz, CDCl₃) 190.3, 144.7, 141.8, 138.1, 135.9, 132.5, 129.1, 129.0, 128.8, 128.7, 128.5, 128.4, 128.3, 127.2, 126.8, 125.2.

(*E*,*E*)-1-(4-Nitrophenyl)-5-phenylpenta-2,4-dien-1-one (**3l**):⁴¹ ¹H NMR (300 MHz, CDCl₃) 8.36-8.32 (m, 2H), 8.12-8.08 (m, 2H), 7.66 (dd, 1H, *J* 8.8 and 1.5 Hz), 7.54-7.50 (m, 2H), 7.43-7.35 (m, 3H), 7.07-7.02 (m, 3H); ¹³C NMR (75 MHz, CDCl₃) 188.9, 149.9, 146.7, 143.6, 143.1, 135.7, 129.7, 129.3, 128.9, 128.6, 127.5, 126.5, 124.5, 123.8, 123.5.

(*E*)-1,3-Diphenylprop-2-en-1-one (**3m**):⁴² IR (KBr) 3056, 1661, 1605, 1576, 1448, 746, 689 cm⁻¹. ¹H NMR (300 MHz, CDCl₃) 8.01-7.97 (m, 2H), 7.77 (d, 1H, *J* 15.9 Hz), 7.55-7.24 (m, 9H); ¹³C NMR (75 MHz, CDCl₃) 189.5, 144.1, 137.6, 134.3, 132.3, 130.0, 128.4, 128.1, 128.0, 128.0, 121.4.

(*E*)-1-(2-Hydroxyphenyl)-3-phenylprop-2-en-1-one (**3n**):⁴³ ¹H NMR (300 MHz, CDCl₃) 12.82 (s, 1H), 7.95-7.91 (m, 2H), 7.69-7.64 (m, 3H), 7.54-7.43 (m, 3H), 7.05-6.93 (m, 2H); ¹³C NMR (75 MHz, CDCl₃) 193.7, 163.6, 145.5,

136.4, 134.6, 130.9, 129.6, 129.0, 128.7, 120.1, 118.8, 118.6.

(*E*)-1-(3-Hydroxyphenyl)-3-phenylprop-2-en-1-one (**3o**):⁴³ ¹H NMR (300 MHz, DMSO-*d*₆): 9.89 (s, 1H), 7.92-7.85 (m, 3H), 7.75 (d, 1H, *J* 15.6 Hz), 7.65 (dd, 1H, *J* 1.5 and 1.1 Hz), 7.50-7.38 (m, 5H), 7.09 (dd, 1H, *J* 2.6 and 0.9 Hz); ¹³C NMR (75 MHz, CDCl₃) 189.5, 169.3, 150.9, 145.5, 139.6, 134.7, 130.7, 129.7, 129.0, 128.5, 126.1, 125.9, 121.7, 121.7.

(*E*)-1-(4-Methoxyphenyl)-3-phenylprop-2-en-1-one (**3p**):³⁹ ¹H NMR (300 MHz, CDCl₃) 8.07-8.02 (m, 2H), 7.80 (d, 1H, *J* 15.7 Hz), 7.66-7.63 (m, 2H), 7.55 (d, 1H, *J* 15.7 Hz), 7.43-7.39 (m, 3H), 7.00-6.96 (m, 2H), 3.88 (s, 3H); ¹³C NMR (75 MHz, CDCl₃) 188.7, 163.4, 143.9, 135.0, 131.0, 130.8, 130.3, 128.9, 128.3, 121.8, 113.8, 55.4.

(*E*)-1-(4-Nitrophenyl)-3-phenylprop-2-en-1-one (**3q**):³⁹ ¹H NMR (300 MHz, CDCl₃) 8.37-8.32 (m, 2H), 8.17-8.12 (m, 2H), 7.85 (d, 1H, *J* 15.6 Hz), 7.69-7.63 (m, 2H), 7.49 (d, 1H, *J* 15.6 Hz), 7.47-7.43 (m, 3H); ¹³C NMR (75 MHz, CDCl₃) 189.0, 150.0, 146.8, 143.0, 134.2, 131.2, 129.4, 129.1, 128.7, 123.8, 121.2.

(*E*)-1-(2-(Allyloxy)phenyl)-3-phenylprop-2-en-1-one (**3r**):⁴⁴ ¹H NMR (300 MHz, CDCl₃) 7.68-7.64 (m, 1H), 7.63-7.56 (m, 2H), 7.49-7.43 (m, 2H), 7.41-7.36 (m, 3H), 7.05 (td, 1H, *J* 7.5 and 1.4 Hz), 6.98 (dd, 1H, *J* 8.2 and 0.7 Hz), 6.10-5.97 (m, 1H), 5.42 (dq, 1H, *J* 2.8 and 1.4 Hz), 5.24 (dq, 1H, *J* 2.8 and 1.4 Hz), 4.64 (dt, 3H, *J* 3.2 and 1.4 Hz); ¹³C NMR (75 MHz, CDCl₃) 192.7, 157.1, 142.7, 135.0, 132.9, 132.5, 130.5, 130.1, 129.5, 128.8, 128.3, 127.1, 120.9, 117.7, 112.8, 69.2.

(*2E*)-3-(2-Furyl)-1-phenylprop-2-en-1-one (**3s**):⁴⁵ IR (film) ν_{\max} /cm⁻¹ 3129, 3067, 1663, 1603, 1552, 1223, 1013, 971, 884, 776; ¹H NMR (300 MHz, CDCl₃) 8.04-7.99 (m, 2H), 7.58 (d, 1H, *J* 15.4 Hz), 7.58-7.51 (m, 1H), 7.50-7.42 (m, 4H), 7.44 (d, 1H, *J* 15.4 Hz); ¹³C NMR (75 MHz, CDCl₃) 189.8, 151.6, 144.9, 132.7, 130.7, 128.5, 128.4, 119.2, 116.3, 112.6.

(*2E*)-3-(2-Furyl)-1-(3-hydroxyphenyl)prop-2-en-1-one (**3t**):⁴⁵ IR (KBr) ν_{\max} /cm⁻¹ 3261, 3128, 1647, 1595, 1551, 1276, 1022, 980, 777; ¹H NMR (300 MHz, CDCl₃) 7.87 (d, *J* 7.8 Hz; 1H), 7.73 (t, 1H, *J* 2.2 Hz), 7.58 (d, 1H, *J* 15.1 Hz), 7.52-7.47 (m, 2H), 7.37 (d, 1H, *J* 15.1 Hz), 7.35-7.28 (m, 1H), 6.71 (d, 1H, *J* 3.4 Hz), 6.49 (dd, 1H, *J* 3.4 and 1.9 Hz), 2.33 (s, 3H); ¹³C NMR (75 MHz, CDCl₃) 189.30, 169.26,

150.81, 145.34, 142.31, 139.59, 135.94, 129.58, 129.28, 128.82, 128.48, 127.29, 126.74, 124.97, 121.55, 125.86, 125.68, 21.06

(*E*)-1-(3-(Allyloxy)phenyl)-3-(furan-2-yl)prop-2-en-1-one (**3u**): ¹H NMR (300 MHz, CDCl₃) 7.63-7.52 (m, 4H), 7.45-7.36 (m, 2H), 7.12 (dd, 1H, *J* 2.6 and 0.7 Hz), 6.71 (d, 1H, *J* 3.4 Hz), 6.50 (dd, 1H, *J* 3.4 and 1.9 Hz), 6.14-6.01 (m, 1H), 5.44 (dq, 1H, *J* 3.1 and 1.5 Hz), 5.31 (dq, 1H, *J* 3.1 and 1.5 Hz), 4.61 (dt, 2H, *J* 3.1 and 1.5 Hz); ¹³C NMR (75 MHz, CDCl₃) 189.2, 158.7, 151.5, 144.8, 139.3, 132.7, 130.5, 129.4, 120.9, 119.7, 119.1, 117.8, 116.2, 113.5, 112.6, 68.7; anal. calcd. for C₁₉H₁₆O₄: C, 74.01; H, 5.23; O, 20.76; found: C, 73.93; H, 5.19; O, 20.88.

Supplementary Information

Data spectra and spectra of synthesized compounds are available free of charge at <http://jbcs.s bq.org.br> as PDF file.

Acknowledgments

We thank the Instituto de Química, Universidade de Brasília, FINEP-CT INFRA No. 970/01, Conselho Nacional de Desenvolvimento Científico e Tecnológico (CNPq), PrP/UEG and FUNAPE/UFU for financial support.

References

- Daskiewicz, J.-B.; Depeint, F.; Viornery, L.; Bayet, C.; Comte-Sarrazin, G.; Comte, G.; Gee, J. M.; Johnson, I. T.; Ndjoko, K.; Hostettmann, K.; Barron, D.; *J. Med. Chem.* **2005**, *48*, 2790.
- Reddy, M. V. B.; Hwang, T.; Leu, Y.; Chiou, W.; Wu, T.; *Bioorg. Med. Chem.* **2011**, *19*, 2751.
- Aponte, J. C.; Castillo, D.; Estevez, Y.; Gonzales, G.; Arevalo, J.; Hammond, G. B.; Sauvain, M.; *Bioorg. Med. Chem. Lett.* **2010**, *20*, 100.
- Dyrager, C.; Wickström, M.; Fridén-Saxin, M.; Friberg, A.; Dahlén, K.; Wallén, E. A. A.; Gullbo, J.; Grotli, M.; Luthman, K.; *Bioorg. Med. Chem.* **2011**, *19*, 2659; Ruan, B.; Lu, X.; Tang, J.; Wei, Y.; Wang, X.; Zhang, Y.; Wang, L.; Zhu, H.; *Bioorg. Med. Chem.* **2011**, *19*, 2688.
- Cheenpracha, S.; Karalai, C.; Ponglimanont, C.; Subhadhirasakul, S.; Tewtrakal, S.; *Bioorg. Med. Chem.* **2005**, *14*, 1710.
- Wattenberg, L. W.; Coccia, J. B.; Galhaith, A. R.; *Cancer Lett.* **1994**, *83*, 165.
- Yoon, G.; Lee, W.; Kim, S.-N.; Cheon, S. H.; *Bioorg. Med. Chem. Lett.* **2009**, *19*, 5155; Monti, S.; Manet, I.; Manoli, F.; Marconi, G.; *Phys. Chem. Chem. Phys.* **2008**, *10*, 6597.

8. Gordon, L. T.; Weitzman, S. A.; *Cancer J.* **1993**, *6*, 257.
9. Wang, Q.; Ding, Z.-H.; Liu, J.-K.; Zheng, Y.-T.; *Antiviral Res.* **2004**, *64*, 189.
10. Quintin, J.; Desrivot, J.; Thoret, S.; Le Menez, P.; Cresteil, T.; Lewin, G.; *Bioorg. Med. Chem. Lett.* **2009**, *19*, 167.
11. Bandgar, B. P.; Gawande, S. S.; Bodade, R. G.; Gawande, N. M.; Khobragade, C. N.; *Bioorg. Med. Chem.* **2009**, *17*, 8168.
12. Sivakumar, P. M.; Kumar, T. M.; Doble, M.; *Chem. Biol. Drug Des.* **2009**, *74*, 68.
13. Vencato, I.; Andrade, C. K. Z.; Silva, W. A.; Lariucci, C.; *Acta Crystallogr., Sect. E: Struct. Rep. Online* **2006**, *62*, o1033; Silva, W. A.; Gatto, C. C.; Oliveira, G. R.; *Acta Crystallogr., Sect. E: Struct. Rep. Online* **2011**, *67*, o2210.
14. Lawrence, N. J.; Rennison, D.; McGown, A. T.; Ducki, S.; Gul, L. A.; Hadfield, J. A.; Khan, N.; *J. Comb. Chem.* **2001**, *3*, 421.
15. *HyperChemTM Professional 7.51*, Hypercube, Inc., 1115 NW 4th Street, Gainesville, Florida 32601, USA.
16. Stewart, J. J. P.; *J. Comp. Chem.* **1989**, *10*, 209.
17. Stewart, J. J. P.; *J. Comp. Chem.* **1989**, *10*, 221.
18. Hohenberg, P.; Kohn, W.; *Phys. Rev.* **1964**, *136*, B864.
19. Kohn, W.; Sham, L.; *Phys. Rev.* **1965**, *140*, A1133.
20. Becke, A. D.; *J. Chem. Phys.* **1993**, *98*, 5648.
21. Lee, C.; Yang, W.; Parr, R. G.; *Phys. Rev.* **1988**, *B37*, 785.
22. Miehlich, B.; Savin, A.; Stoll, H.; Preuss, H.; *Chem. Phys. Lett.* **1989**, *157*, 200.
23. Frisch, M. J.; Trucks, G. W.; Schlegel, H. B.; Scuseria, G. E.; Robb, M. A.; Cheeseman, J. R.; Scalmani, G.; Barone, V.; Mennucci, B.; Petersson, G. A.; Nakatsuji, H.; Caricato, M.; Li, X.; Hratchian, H. P.; Izmaylov, A. F.; Bloino, J.; Zheng, G.; Sonnenberg, J. L.; Hada, M.; Ehara, M.; Toyota, K.; Fukuda, R.; Hasegawa, J.; Ishida, M.; Nakajima, T.; Honda, Y.; Kitao, O.; Nakai, H.; Vreven, T.; Montgomery, J. A. Jr.; Peralta, J. E.; Ogliaro, F.; Bearpark, M.; Heyd, J. J.; Brothers, E.; Kudin, K. N.; Staroverov, V. N.; Kobayashi, R.; Normand, J.; Raghavachari, K.; Rendell, A.; Burant, J. C.; Iyengar, S. S.; Tomasi, J.; Cossi, M.; Rega, N.; Millam, J. M.; Klene, M.; Knox, J. E.; Cross, J. B.; Bakken, V.; Adamo, C.; Jaramillo, J.; Gomperts, R.; Stratmann, R. E.; Yazyev, O.; Austin, A. J.; Cammi, R.; Pomelli, C.; Ochterski, J. W.; Martin, R. L.; Morokuma, K.; Zakrzewski, V. G.; Voth, G. A.; Salvador, P.; Dannenberg, J. J.; Dapprich, S.; Daniels, A. D.; Farkas, Ö.; Foresman, J. B.; Ortiz, J. V.; Cioslowski, J.; Fox, D. J.; *Gaussian 09, Revision A.1*; Gaussian, Inc.: Wallingford, CT, USA, 2009.
24. Fukui, K.; *Theory of Orientation and Stereoselection*; Springer-Verlag: New York, 1975, p. 34.
25. *Einsight 3.0 Infometrix*, Suite 833; Infometrix, Inc.: Seattle, WA, USA, 1991.
26. Sharaf, M. A.; Illman, D. L.; Kolwalski, B. R.; *Chemometrics*; Wiley: New York, USA, 1986.
27. Brereton, R. G.; *Chemometrics: Data Analysis for the Laboratory and Chemical Plant*; Wiley: Chichester, USA, 2003.
28. National Committee for Clinical Laboratory Standards (NCCLS); *Methods for Dilution Antimicrobial Susceptibility Tests for Bacteria that Grow Aerobically: Approved Standard, M7-A55th*, 5th ed.; NCCLS: Wayne, PA, 2000.
29. Ellof, J. N.; *Planta Medica* **1998**, *64*, 711.
30. Kusucu, C.; Rapino, B.; McDermott, L.; Hadley, S.; *J. Clin. Microbiol.* **2004**, *42*, 1224.
31. Enraf-Nonius; *CAD-4/PC Software*, version 1.2; Enraf-Nonius: Delft, The Netherlands, 1993.
32. Sheldrick, G. M.; *SHELXS97 and SHELXL97*; University of Göttingen: Germany, 1997.
33. Macrae, C. F.; Edgington, P. R.; McCabe, P.; Pidcock, E.; Shields, G. P.; Taylor, R.; Towler, M.; van de Streek, J.; *J. Appl. Cryst.* **2006**, *39*, 453.
34. Johnson, C. K.; *ORTEP-II: a FORTRAN Thermal-Ellipsoid Plot Program for Crystal Structure Illustrations*; Oak Ridge National Laboratory Report ORNL-5138: Tennessee, USA, 1976.
35. Farrugia, L. J.; *J. Appl. Cryst.* **1997**, *30*, 565.
36. Chiaradia, L. D.; Mascarello, A.; Purificação, M.; Vernal, J.; Cordeiro, M. N. S.; Zenteno, M. E.; Villarino, A.; Nunes, R. J.; Yunes, R. A.; Terenzi, H.; *Bioorg. Med. Chem. Lett.* **2008**, *18*, 6227.
37. Buu-Hoi, Ng. Ph.; Loc, T. B.; Xuong, Ng. D.; *Bull. Soc. Chim. Fr.* **1955**, 694.
38. Solhy, A.; Tahir, R.; Sebti, S.; Skouta, R.; Bousmina, M.; Zahmely, M.; Larzek, M.; *Appl. Catal., A* **2010**, *374*, 189.
39. Zhu, Y.-W.; Yi, W.-B.; Cai, C.; *J. Fluorine Chem.* **2011**, *71*.
40. Pang, S.; Jian, F.; Xuan, Z.; Wang, J.; *Crystal Growth Des.* **2009**, *9*, 43.
41. Santos, C. M. M.; Silva, A. M. S.; Cavaleiro, J. A. S.; Lévai, A.; Patonay, T.; *Eur. J. Org. Chem.* **2007**, 2877.
42. Hayat, F.; Salahuddin, A.; Umar, S.; Azam, A.; *Eur. Med. Chem.* **2010**, *45*, 4669.
43. Karki, R.; Thapa, P.; Kang, M. J.; Jeong, T. C.; Namb, J. M.; Kim, H.-L.; Na, Y.; Cho, W.-J.; Kwon, Y.; Lee, E.-S.; *Bioorg. Med. Chem.* **2010**, *18*, 306.
44. Saito, T.; Nagashima, M.; Karakasa, T.; Motoki, S.; *J. Chem. Soc. Chem. Commun.* **1992**, 411.
45. Cetin, A.; Cansiz, A.; Digrak, M.; *Heteroat. Chem.* **2003**, *14*, 345.
46. Zhao, P.-L.; Liu, C.-L.; Huang, W.; Wang, Y.-Z.; Yanga, G.-F.; *J. Agric. Food Chem.* **2007**, *55*, 5697.

Submitted: September 21, 2012

Published online: February 19, 2013